Magnetoresistance Spectroscopy of Near-Surface Defects in Semiconducting Hosts

S. R. McMillan[1]

[1] *Donostia International Physics Center (DIPC), E-20018, Donostia-San Sebastián, Spain*

Components for quantum information processing and quantum sensing require localized spin-coherent states. These states can be realized in isolated magnetic dopants embedded in a non-magnetic semiconducting host. A critical requirement for utilizing a dopant-based system is an understanding of how the complex host environment influences the coherent spin dynamics at an individual site. Resolving these faint dynamics against a strong incoherent background is a challenge that is typically solved by exciting the system via ac fields. In this work we propose a method that leverages non-equilibrium spin correlations in the presence of dc magnetic fields to probe coherent interactions in individual near-surface magnetic dopants. In previous work, we calculate the dc magnetoresistance through a spin-1/2 dopant that is addressed by a spin-polarized scanning tunneling microscope (SP-STM) and exchange coupled to an inert spin-1/2 center [1]. This work is then extended to the technologically relevant case of an individual spin-1 center [2]. In particular we use the stochastic Liouville formalism to calculate the current through a divacancy in 4H-SiC. We predict distinct few-milli-tesla-dc magnetoresistance signatures that identify a *single* spin-triplet center's character and reveal the orientation of the spin triplet's zero-field splitting axis relative to the magnetic contact's polarization. For example, in 4H-SiC the single *(hh)*, *(kk)*,*(hk)*, and *(kh)* divacancies are all distinct. Spin-polarized current flow efficiently polarizes the spin, potentially electrically initializing spin-triplet-based qubits without the use of ac fields or optical hardware.

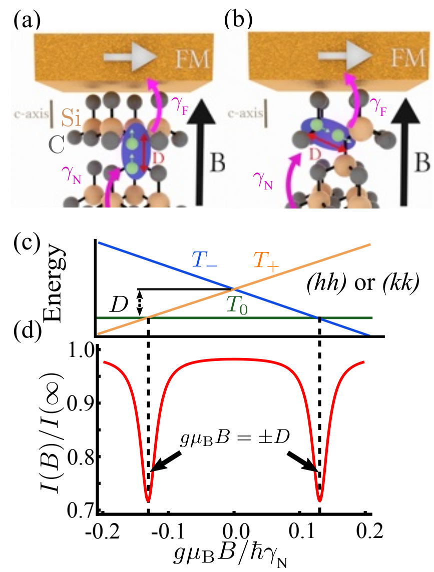

Figure 1. Schematic current path for an electron through a (a) *(kk)* divacancy or (b) basal *(kh)* divacancy in 4H-SiC. The applied magnetic field **B** (black), and hopping rates (pink), as well as the axis of the zero-field splitting *D* (red double-ended arrow). (c) Energy eigenstates for the divacancy in (a). (d) inverse MR for (a).

[1] S. R. McMillan *et al.*, Phys. Rev. Lett. **125**, 257203(2020).
[2] S. R. McMillan and M. E. Flatté, arXiv:2112.14805.

+ Author for correspondence: stephen.r.mcmillan@proton.me

Supplementary Information:

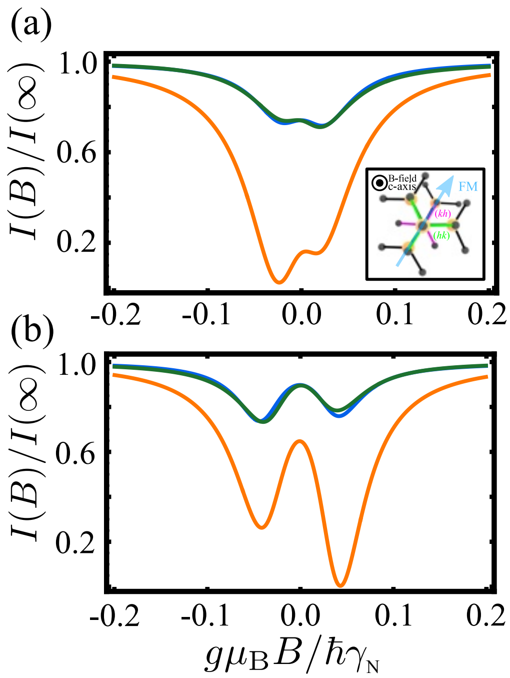

Figure 2. (a) MR for *(kh)* divacancies with azimuthal angle of 0 (orange), $2\pi/3$ (blue), and $4\pi/3$ (green) relative to the FM magnetization. (b) MR for *(hk)* divacancy with azimuthal angle of $\pi/3$ (blue), π (orange), and $5\pi/3$ (green). For both $\gamma_F/\gamma_N = 0.02$. Inset: sketch of *(kh)* and *(hk)* divacancy orientation and the FM magnetization viewed along the *c*-axis.

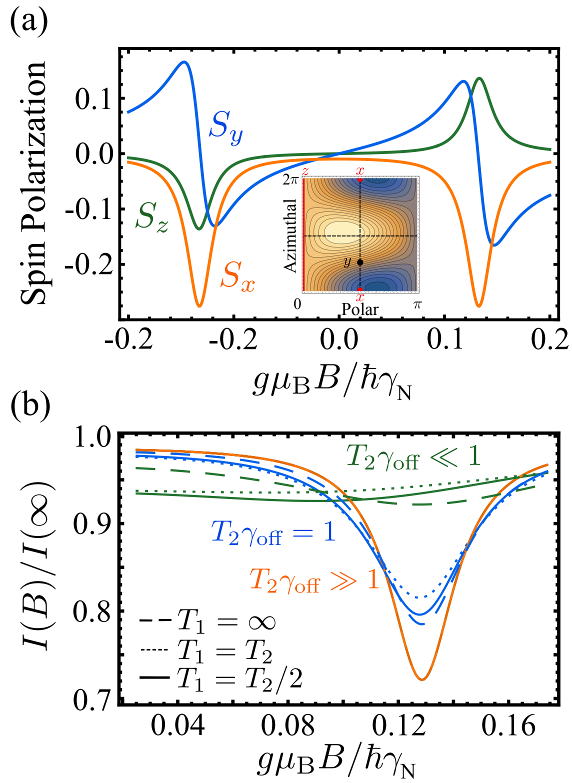

Figure 3.(a) Spin polarization of *(hh)* divacancy. (Inset) contour plot of $B>0$ total spin polarization, with light color indicating a maximum. Points of interest are labeled in the defect orientation basis. $\hat{z} \parallel$ defect axis and $\perp$ to the interface, with FM polarization $\parallel \hat{x}$. The maximum polarization is 0.3 along the $(\theta, \phi) = (1.11, 3.26)$ direction. (b) Positive field current dip of *(hh)* divacancy with negligible (orange, $T_2\gamma_N = 10^5$), considerable (blue, $T_2\gamma_N = 100$), and substantial (green, $T_2\gamma_N = 10$) on-site decoherence, assuming three different T_1's. Decoherence broadens the signal whereas finite T_1 shifts to smaller B. $\gamma_F/\gamma_N = 0.02$.

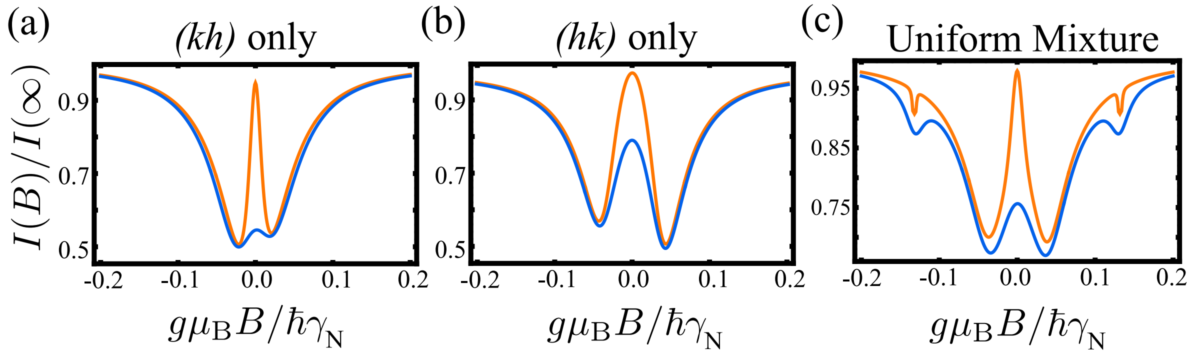

Figure 4.Ensemble magnetoresistance for a uniform distribution of *(kh)* (a), *(hk)* (b), and each of the four (c) divacancies for two different hopping ratios: $\gamma_{\mathrm{F}}/\gamma_{\mathrm{N}} = 0.02$ (blue) and $\gamma_{\mathrm{F}}/\gamma_{\mathrm{N}} = 0.002$ (orange).